AIAA JOURNAL
Vol. 34, No. 11, November 1996

Controlled Leading-Edge Suction for Management of Unsteady Separation over Pitching Airfoils

Mah'd Alrefai* and Mukund Acharya†
Illinois Institute of Technology, Chicago, Illinois 60616

The effect on the unsteady surface pressures of controlled suction from a spanwise slot, located at 2% chord in the suction surface of a two-dimensional NACA 0012 airfoil model, was examined in detail for a wide range of pitch rates with a constant velocity ramp motion. The experiments were conducted in the Andrew Fejer Wind Tunnel at the Illinois Institute of Technology's Fluid Dynamics Research Center. The optimum suction required to meet three different control objectives, suppression of the dynamic-stall vortex, delaying detachment of the vortex from the airfoil surface, and maximizing the unsteady lift, was determined for different pitch rates and angles of attack. The pressure data were used to develop specifications for the flow state over the airfoil surface that would meet these objectives. Such specifications are necessary for the development of on-line flow management systems. A procedure was also developed to account for variations in suction and motion history.

Nomenclature

C_l = lift coefficient
C_p = pressure coefficient, $2(p - p_\infty)/(\rho U_\infty^2)$
c = airfoil chord length
p = surface pressure
p_∞ = reference static pressure
Q = dimensionless suction flow rate, $\dot{Q}_s/(U_\infty c^2)$
Q_{opt} = optimum suction rate for a given objective
$\dot{Q}_s$ = volumetric suction flow rate
Re_c = chord Reynolds number, $U_\infty c/\nu$
S = surface vorticity flux, $(1/\rho)(\partial p/\partial s)$
S^+ = dimensionless surface vorticity flux, $2cS/U_\infty$
s = coordinate along airfoil surface
t_p = time period for pitch-up motion through an angle $\Delta\alpha$
U_∞ = freestream velocity
α = angle of attack
α^+ = dimensionless pitch rate, $(\Delta\alpha c)/(t_p U_\infty)$
$\Delta\alpha$ = change in angle of attack during pitch up
ρ = fluid density
ν = fluid kinematic viscosity

Introduction and Background

THE development of a new generation of aircraft with increased maneuverability, allowing operation at higher maximum pitch and roll rates and at higher angles of attack than currently possible, will require effective on-line systems to control the unsteady flowfield that develops over the wings. The control strategy must be based on a knowledge of the unsteady flow behavior that is dominated by leading-edge separation and processes that occur subsequently, such as the formation of a dynamic-stall vortex. Investigations at the Illinois Institute of Technology (IIT) and elsewhere have led to a reasonably good understanding of these phenomena. Recent experiments at IIT[1–4] have provided several important insights into the development of the unsteady separation in the leading-edge region of two-dimensional airfoils undergoing a pitch-up motion.

An important result is that the formation of the dynamic-stall vortex is dependent on the accumulation of reverse-flow fluid in the leading-edge region of the suction surface. Karim and Acharya[5] developed one possible strategy for altering the unsteady flow development and the formation of the dynamic-stall vortex. Their approach was to control the accumulation of reverse-flow fluid in the leading-edge region of the airfoil suction surface by removing fluid at a specified rate through a suction slot located in the suction surface near the leading edge, at about 2% of chord. Figure 1 shows a typical result from their experiments. It can be argued that removal of all this fluid, at the rate at which it arrives in the leading-edge region, would prevent lift-up of the shear layer and hence prevent vortex formation altogether. Alternatively, partial removal of the reverse-flow fluid would reduce the accumulation rate, thereby resulting in a delay of the formation of the dynamic-stall vortex and/or a change in its size and strength. Karim and Acharya[5] described experiments that were carried out to investigate the validity of these arguments and the feasibility and limitations of this approach to suppress, modify, or otherwise control the dynamic-stall vortex. Their results confirmed that controlling the reverse-flow accumulation is

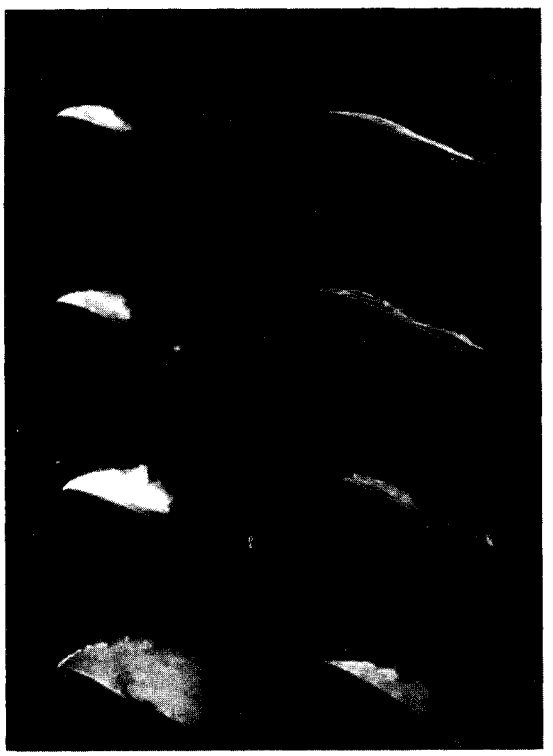

Fig. 1 Effect of suction on the development of the dynamic-stall vortex[5]; $\alpha^+ = 0.15$ and $Q = 0.004$.

Presented as Paper 95-2188 at the AIAA 26th Fluid Dynamics Conference, San Diego, CA, June 19–22, 1995; received Dec. 2, 1995; revision received June 18, 1996; accepted for publication July 5, 1996; also published in *AIAA Journal on Disc*, Volume 2, Number 1.

*Graduate Research Assistant, Fluid Dynamics Research Center.
†Professor, Fluid Dynamics Research Center. Senior Member AIAA.

indeed the key to management of the leading-edge separation and the dynamic-stall vortex. The parameters that provide a measure of control were identified, and the variation of these parameters with pitch rate, angle of attack, and Reynolds number was investigated. Details of the flow response to control action, as well as the applicability and limitations of leading-edge suction as an unsteady flow management tool, were determined for a range of pitch rates and chord Reynolds numbers.

There have been a few computational efforts to model flow control over unsteady airfoils using suction or injection. For instance, Yang et al.[6] described control of the dynamic-stall vortex using modulated suction and injection at the airfoil surface, over an area that varies with the dimensionless pitch rate. Their computational results showed a delay in the onset of dynamic stall, with a corresponding increase in lift and reduction of drag.

Objectives

The objectives of this work were to investigate controlled leading-edge suction in more detail, and to assess its applicability as an actuator in a flow-control system designed for flow management strategies with different objectives. Three objectives were examined: suppression of the dynamic-stall vortex, delaying detachment of the vortex from the airfoil (thereby delaying dynamic stall), and optimizing the unsteady lift during a maneuver. Other objectives (for example, limiting the pitching moment) might be useful as well, but these were not examined in this study. The data generated were used by Kawthar-Ali and Acharya[7] for the development and training of a neural-network-based controller that will be part of a prototype feedback control system.

Experimental Arrangement

Wind Tunnel

The experiments were conducted in the Andrew Fejer Unsteady Wind Tunnel at IIT's Fluid Dynamics Research Center. This is a closed-circuit, low-speed facility driven by an axial-vane fan powered by a 40-hp synchronous motor. The wind-tunnel test section is 0.61×0.61 m in cross section and 3.1 m in length. Flow velocities up to 40 m/s can be reached by adjusting a magnetic clutch excitation that controls the fan rotational speed. Screens, honeycombs, and a contraction region upstream of the test section yield a turbulence level of 0.03% at the maximum velocity. A controlled, unsteady motion can also be imparted to a model positioned in the flow.

Airfoil Model

The airfoil model was the same as that used by Metwally[1] and Karim and Acharya.[5] It had a NACA 0012 profile with a chord length of 30 cm, a thickness of 12% chord, and a span of 60 cm and was equipped for surface-pressure measurements. Details of its design and construction are described by Metwally.[1] A special feature of the airfoil design provided the ability to withdraw fluid from a spanwise suction slot, 0.5 mm wide, placed at 2% chord in the suction surface. A suction chamber with a volume of 50 cm^3 was built into the leading-edge region and connected to the slot. The airfoil was mounted in the horizontal midplane of the test section, allowing it to pitch about its quarter-chord pivot line. The model was driven by a low-inertia, high-torque, servo-controlled dc motor with an analog servo-amplifier. A Schaevitz R30D rotary-variable-differential transformer provided a signal proportional to the airfoil angular position.

Suction System

The airfoil suction chamber was divided into five compartments to achieve uniform suction across the span. These compartments were connected by flexible tubes to a circular distributor located inside the airfoil. The distributor was connected to an evacuated tank located outside the tunnel through a high-vacuum, direct-acting solenoid valve. A flow meter was mounted between the distributor and the solenoid valve. The latter was actuated by signals from a personal computer to enable suction through the leading-edge slot at predetermined angles while the airfoil was in motion. The vacuum tank was evacuated to a specified vacuum level before each experimental run to obtain the desired suction flow rate.

Procedure, Instrumentation, and Measurements

The evolution of the unsteady pressure field was studied for a range of pitch rates ($0.01 < \alpha^+ < 0.15$) and suction flow rates ($0 < Q < 24 \times 10^{-3}$). These measurements were supplemented with a limited amount of flow visualization to examine the state of the flow over the suction surface for selected conditions. The unsteady pressure data were used to obtain ensemble-averaged, chordwise pressure distributions, surface-vorticity-flux distributions, and unsteady lift coefficients. Tests showed that an ensemble of three realizations was sufficient.

Unsteady pressure measurements were made using a Setra model 239 pressure transducer together with a Scanivalve system. The transducer, tubing, etc., together had the required frequency response for these measurements.[1] The uncertainty in the pressure data reported in this paper was estimated using standard techniques to be ±2.3%. A trapped-vortex-pair flow meter was used to measure the volumetric suction flow rates. The uncertainty in the suction flow rate measurements was estimated to be ±3%, whereas the uncertainty in the measurement of freestream velocity was 0.2%. The model motion was a hold-pitch-hold ramp-up from 0 to 45 deg at a constant angular velocity. Unless otherwise stated, a constant suction was applied between 6 and 38 deg angles of attack. Further details of the instrumentation and procedures are in Alrefai.[8]

Results and Discussion

Effect of Suction on the Surface-Pressure Distributions

The effect of leading-edge suction on the evolution of the unsteady surface pressures and flow development over the suction surface was examined by varying the suction flow rate systematically while keeping other parameters constant. Figures 2–4 show the chordwise variation of the surface-pressure coefficient C_p over the airfoil for three angles of attack: 26, 29, and 35 deg. Locations along the suction and pressure surfaces are designated by positive and negative values of x/c, respectively. In each case, the dimensionless pitch rate $\alpha^+ = 0.15$, the chord Reynolds number was 1.1×10^5, and pressure distributions are shown for 10 different flow rates Q varying from 0 (the natural case with no suction applied) to 0.01364. Flow visualization showed that at $\alpha^+ = 0.15$, with no suction applied, the dynamic-stall vortex was well formed at an angle of attack of 26 deg, had begun to move across the suction surface by 29 deg, and had detached and started to convect off the airfoil by 35 deg. The pressure distributions at these angles for $Q = 0$ in Figs. 2–4 are consistent with this sequence of flow development. The presence and extent of the dynamic-stall vortex over the suction surface are indicated in the pressure distributions by a broad suction peak, known as the dynamic-stall vortex peak (DSVP). It first appears between 5 and 15% of chord, the location at which the vortex forms, and its minimum is indicative of the vortex center. As the vortex grows, detaches from the airfoil surface, and convects off the airfoil, a corresponding broadening and movement of the DSVP is observed. This movement of the vortex with increase in angle of attack is clearly reflected in the behavior of the DSVP for $Q = 0$ in Figs. 2–4. The suction-surface pressure distribution usually contains another peak, referred to as the leading-edge suction peak (LESP). As seen in the figures, this peak occurs over a very narrow spatial region of the surface between 0 and 3% chord as the airfoil pitches up and is associated with the acceleration of the flow around the leading edge.

Application of suction delays or inhibits formation of the dynamic-stall vortex. The effect of this suction on the flow development and the associated surface-pressure distribution varies with the angle of attack, as one would expect from the results of Karim and Acharya.[5] At each of the angles of attack shown in Figs. 2–4, similar trends were observed with gradual increase in the magnitude of Q. At first, the DSVP becomes more compact and remains further upchord. With further increase in Q, there comes a point when the DSVP is no longer seen. Increase in Q beyond this value does not significantly affect the pressure distribution, other than to increase the magnitude of the LESP. An examination of the data shown in Figs. 2–4 in conjunction with flow visualization photographs revealed that the minimum value of Q required to suppress the dynamic-stall vortex completely at an angle of attack of 26 deg was 0.0017, whereas the values were 0.0028 and 0.0074 at 29 and

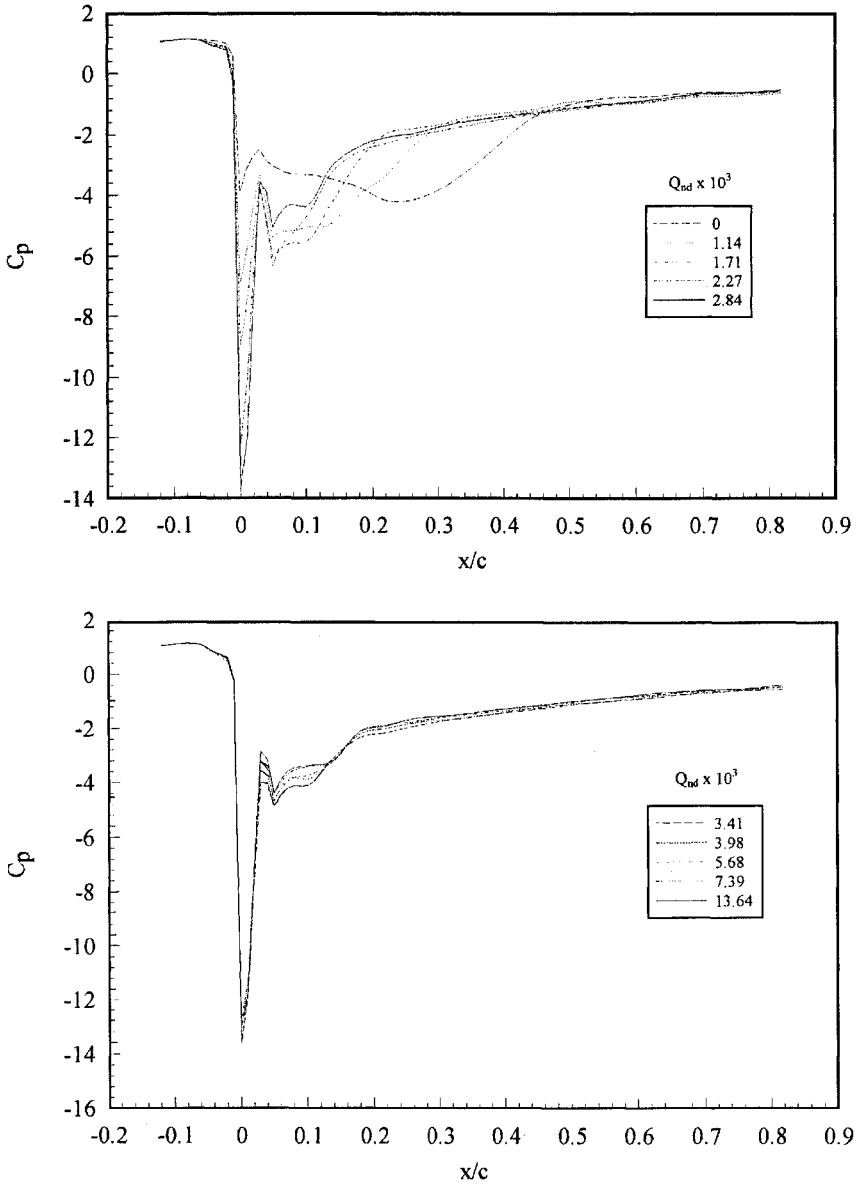

Fig. 2 Variation of chordwise surface-pressure coefficient with suction; $\alpha^+ = 0.15$ and $\alpha = 26$ deg.

35 deg, respectively. The pressure data also showed that in each of these cases suction at rates higher than the values specified resulted only in increasing the leading-edge suction peak, whereas suction at levels lower than those specified allowed the vortex to form to varying extents, depending on the magnitude of the parameters.

Data obtained at other angles of attack at this pitch rate, as well as measurements at other pitch rates, exhibited very similar trends, except that the values of Q at which different states were observed varied with α and α^+. These results are discussed in detail by Alrefai.[8] The observations can be summarized as follows: at a given pitch rate and angle of attack, complete suppression of the dynamic-stall vortex could be achieved by increasing the suction rate until an optimum suction rate (Q_{opt}) was reached. Any further increase in the suction rate had no effect on the flowfield or pressure distribution, except to increase the magnitude of the LESP. Suction at rates less than optimum resulted in the presence of a dynamic-stall vortex whose size and location varied with the suction applied or in a separated flowfield established after the vortex had convected off the airfoil.

The minimum suction rate necessary to suppress the dynamic-stall vortex, Q_{opt}, decreased as α^+ increased or α decreased. The criterion described earlier was used to determine Q_{opt} for the five dimensionless pitch rates examined, over the full range of angle of attack for which the vortex was completely suppressed. The result is shown in Fig. 5. Note that $Q = 24 \times 10^{-3}$ corresponded to the upper limit of the suction system.

It is evident from the pressure distributions of Figs. 2–4 that the optimum suction needed to delay detachment of the vortex or to maximize the lift at any angle of attack is different from that required to suppress the dynamic-stall vortex completely. The optimum suction required for these control objectives was also determined in a similar fashion.

Specification of Flow State

A central issue in active control of such flows is the identification of flow state. A determination of the flow state must be made from a measurement of some property of the flow and then compared with the state desired to decide whether any action is needed to alter the flow state. To be effective for this purpose, the property or variable to be monitored must be measurable with ease; for instance, measurements to obtain velocity-field information might prove difficult or expensive to incorporate in a practical feedback control system.

The variable that presents the most practical alternative for flow-state identification is surface pressure. The signatures of the desired flow states discussed earlier are discernible in the suction-surface pressure distributions, allowing use of the latter for identification of the flow state. Data such as those shown in Figs. 2–4 demonstrated that an examination of comparative pressure levels and pressure

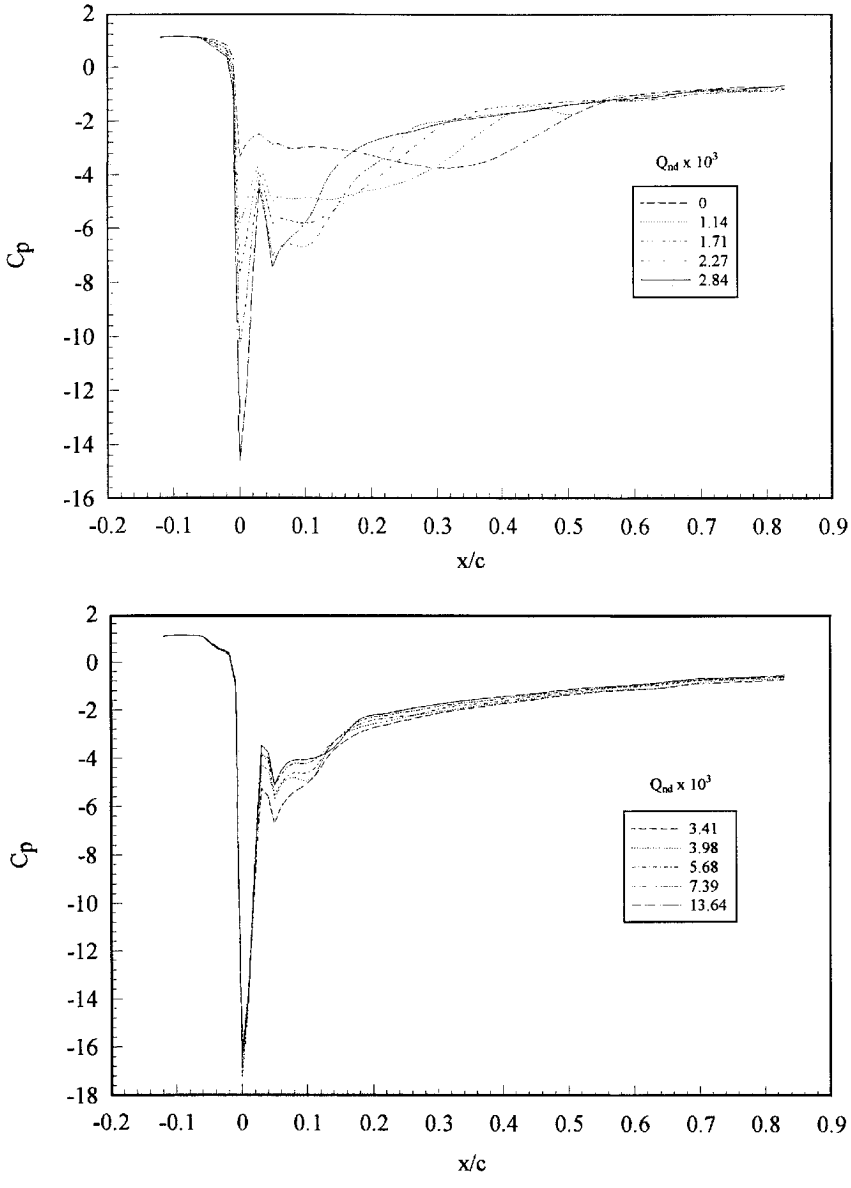

Fig. 3 Variation of chordwise surface-pressure coefficient with suction; $\alpha^+ = 0.15$ and $\alpha = 29$ deg.

gradients from measurements at a few discrete locations in the leading-edge region of the suction surface between 0 and 10% chord can be used to indicate different states of the flow over the suction surface; e.g., a flow state where the dynamic-stall vortex is suppressed or a state where the vortex is still bound to the airfoil surface.

Suppression of the Dynamic Stall Vortex

An examination of the surface-pressure data showed that the pressure distribution in the region between 4 and 15% chord provided an excellent indication of the flow states corresponding to a fully suppressed vortex (achieved when $Q \geq Q_{\text{opt}}$). A typical example is shown in Fig. 6, where the pressure distributions with $Q = Q_{\text{opt}}$ are shown for the five pitch rates at an angle of attack of 20 deg. Beyond $x/c = 0.16$, the data collapsed reasonably well. Between 0 and 4% of chord, a systematic increase in the LESP magnitude was seen with decreasing pitch rate. In the region between 4 and 15%, trends in the pressure variations were very similar, with a small but detectable increase in the magnitude of C_p as α^+ decreased. Similar results were obtained at other angles of attack where suction could be used to suppress the vortex; the data showed a small, systematic increase in the magnitude of C_p in this region with increase in the angle of attack. The nature of variations in the surface pressure over this region with a suppressed vortex was clearly distinguishable from trends in the pressure for all other states. This observation enabled the development of a specification for the required pressure field in the region between 4 and 15% of chord that would ensure a flow state over the suction surface consistent with a suppressed dynamic-stall vortex.

Delaying Dynamic-Stall Vortex Detachment

To develop a criterion that describes the state of flow with an attached dynamic-stall vortex, the unsteady pressure distributions were examined together with the surface vorticity flux S computed using spline fits to the pressure data. The range of interest was restricted to the first 15% of the chord. The results are summarized with the aid of Fig. 7. The variation of the dimensionless vorticity flux S^+ is shown in Fig. 7a for $\alpha^+ = 0.01$ and an angle of attack of 12 deg. (Note that S and S^+ represent the surface-vorticity flux only in the absence of surface transpiration. This requirement holds true at all points of the airfoil surface except at the suction slot location. However, S and S^+ may also be viewed as the spatial pressure gradient without affecting any of the conclusions.) Two prominent features were observed for all of the suction rates used: a positive peak at 2% chord and a negative peak at about 4% chord. The corresponding pressure distributions showed that the vortex was still attached to the airfoil surface, even for the natural case (no suction). At an angle of attack of 18 deg, the pressure data showed that the vortex was suppressed at suction rates 5.68×10^{-3}, 11.37×10^{-3},

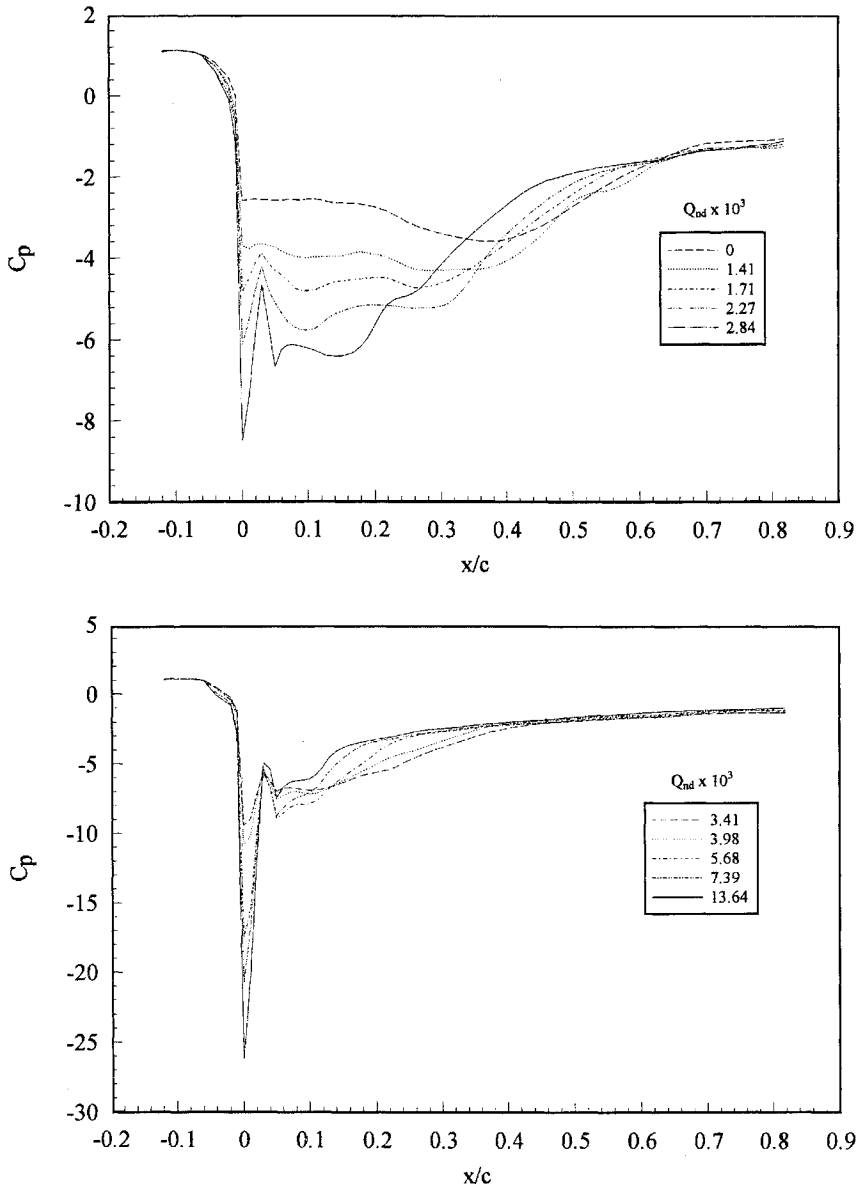

Fig. 4 Variation of chordwise surface-pressure coefficient with suction; $\alpha^+ = 0.15$ and $\alpha = 35$ deg.

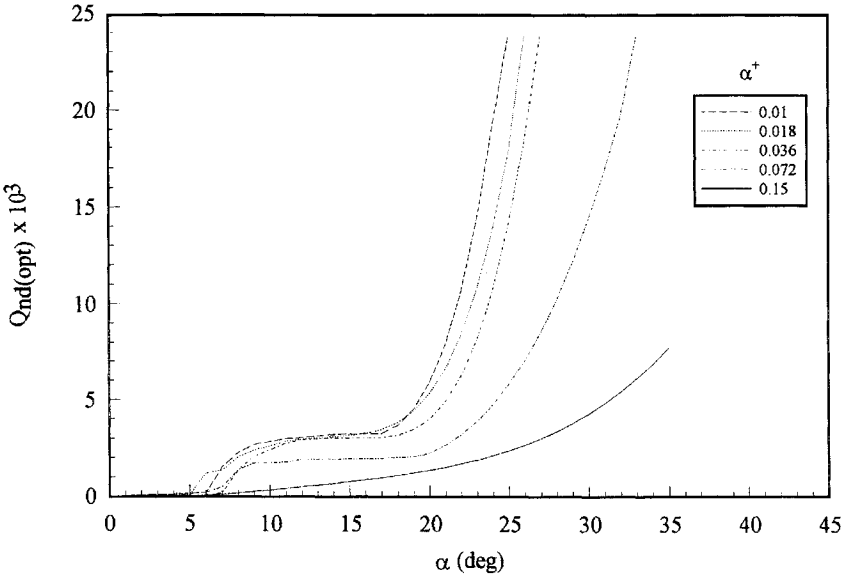

Fig. 5 Variation of optimum suction for suppression of the dynamic-stall vortex.

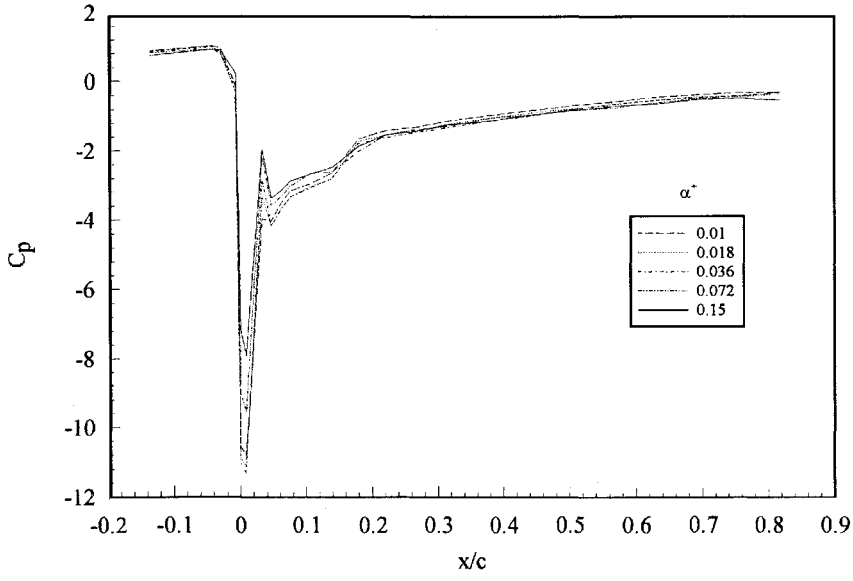

Fig. 6 Pressure distributions at different pitch rates with a suppressed dynamic-stall vortex; α = 20 deg.

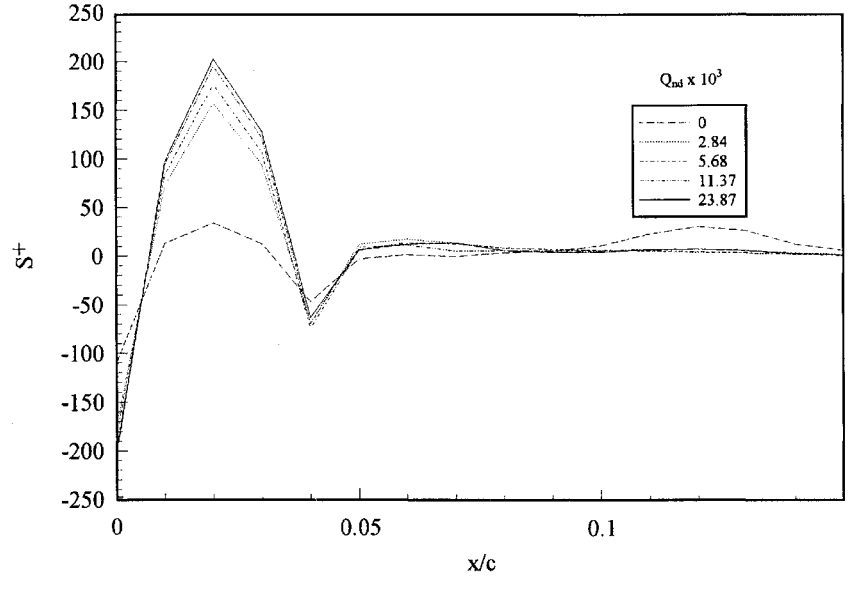

Fig. 7a Vorticity-flux distributions at different suction flow rates; α^+ = 0.01 and α = 12 deg.

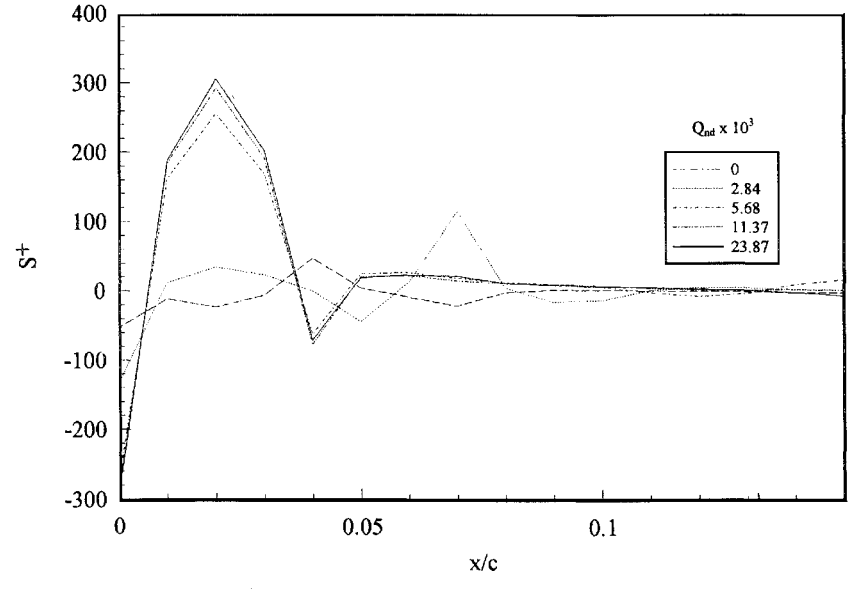

Fig. 7b Vorticity-flux distributions at different suction flow rates; α^+ = 0.01 and α = 18 deg.

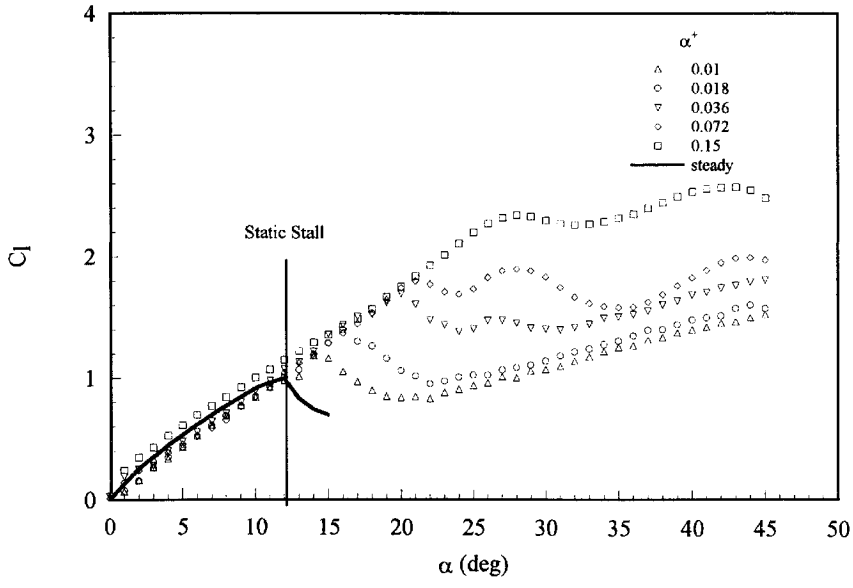

Fig. 8 Variation of lift coefficient with pitch rate.

and 23.87×10^{-3}, whereas at 2.84×10^{-3} the vortex had formed and remained attached to the surface and for $Q = 0$ the vortex had detached from the airfoil. The corresponding vorticity flux variations in Fig. 7b show positive peaks at 2% and negative peaks between 4 and 5% for all cases except $Q = 0$. An examination of plots such as these for all of the pitch rates and angles of attack showed that a positive peak with an S^+ magnitude of 20 or greater at 2% chord coexisted with a negative peak between 4 and 5% chord only for flow states with either a suppressed or attached vortex.

This observation can be used as a criterion to identify a flow state where the vortex has not detached from the airfoil surface. In addition, the optimum suction flow rate to delay detachment of the dynamic-stall vortex may be defined as the minimum value of Q that satisfies the preceding criterion.

Optimizing the Unsteady Lift

The pressure data acquired at different suction and pitch rates were integrated to determine the lift-coefficient variation with angle of attack. Figure 8 shows these variations as a function of angle of attack for the natural case (no suction) for the five pitch rates investigated. The steady-state $C_l - \alpha$ curve is also shown for comparison. In all cases, the lift coefficient increased beyond the static stall value, reaching a peak whose magnitude increased with pitch rate. Beyond this peak, the lift decreased because of the onset of dynamic stall. Note that blockage and three-dimensional effects could be significant at the higher angles of attack, thereby affecting some of the measured quantities. Indeed, this is reflected in the shape of the lift curves in Fig. 8. However, this does not affect the conclusions in any fundamental way.

The effect of suction on the lift coefficient for $\alpha^+ = 0.15$ is shown in Fig. 9a. Increase in suction resulted in a systematic shift of the peak value of C_l to higher angles of attack, from 28 deg with $Q = 0$ to 38 deg for $Q = 5.68 \times 10^{-3}$. Continuation of this trend is highly likely but could not be confirmed because suction was turned off at 38 deg.

The effect of suction rate on the magnitude of C_l was interesting. When the angle of attack was lower than the value for the onset of dynamic stall with no suction, the lift decreased with increasing suction, since the effect of suction was either to reduce the size of the vortex or to suppress it partially or completely. At angles of attack greater than this value, the lift first increased with suction rate and beyond a certain point decreased as suction was increased further. In this case, suction initially served to delay detachment of the vortex, thereby providing increased lift. Beyond a certain magnitude of suction, however, the suction started to reduce the size of the vortex, and the lift decreased. An examination of the corresponding pressure distributions supported this explanation. The amount of suction needed to maximize the lift gradually increased with the angle of attack. With decrease in pitch rate, the effects were similar; however, both the maximum values of C_l and the angles of attack at which these occurred decreased as the pitch rate decreased. The behavior at $\alpha^+ = 0.018$ is shown in Fig. 9b. Results for the other pitch rates are discussed by Alrefai.[8]

Comparison of Suction Requirements

The minimum suction (i.e., Q_{opt}) required at any pitch rate and angle of attack varied with the objective. Not surprisingly, Q_{opt} was the largest for complete vortex suppression. The magnitude needed to maximize the lift was smaller, whereas that required to delay dynamic-stall vortex detachment was the smallest. Figure 10 shows the surface-pressure distributions and the corresponding magnitudes of Q_{opt} for the three objectives for $\alpha^+ = 0.15$ and $\alpha = 35$ deg. The variation of Q_{opt} with angle of attack for each objective at a constant pitch rate of 0.15 is shown in Fig. 11. For each objective, Q_{opt} increased with angle of attack and decreased with pitch rate.

Effect of Motion and Suction History

In these experiments, a constant-velocity ramp motion from 0 to 45 deg was used, together with a constant suction flow rate applied between angles of attack of 6 and 38 deg during pitch up. An important assumption was made in interpreting the results: for a given angle of attack α and pitch rate α^+, the net influence of the past motion and suction history is to determine the flow state at that (α, α^+), as measured by the pressure distribution. The results of the present experiments should therefore be valid for any prior motion of the airfoil and suction history up to that instant, provided that the surface-pressure distribution at that value of (α, α^+) can be matched to one from the present experiments at the same (α, α^+), even if the instantaneous suction flow rate is different. In fact, the likelihood is that the suction flow rates would generally be different. If this condition is met, the pressure data generated in the present experiment may be used to determine the change ΔQ in suction required to change the flow state at that (α, α^+), as measured by the pressure distribution, from one condition to another.

To assess the validity of this assumption, experiments were carried out to modify the motion history by the use of a dual-ramp motion in which the airfoil velocity was changed from one constant value to another at an intermediate angle during pitch up. Two motion profiles—a slow ramp/fast ramp combination and a fast ramp/slow ramp combination—were used. The suction flow rate used through the entire motion was kept constant at a value Q_i. The pressure distribution over the airfoil surface at a selected angle of attack during the second phase of the dual-ramp motion was compared with the pressure distributions at the same pitch rate and angle of attack, but

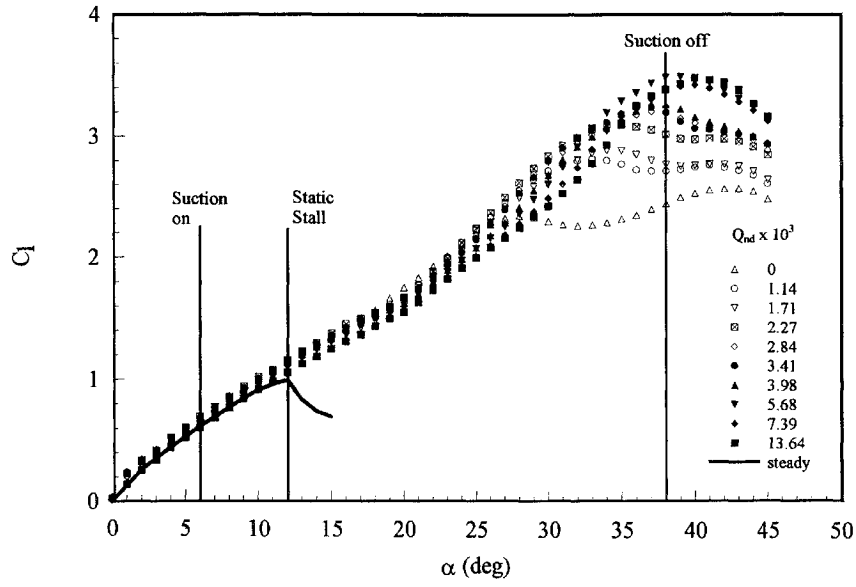

Fig. 9a Effect of suction on the lift coefficient; $\alpha^+ = 0.15$.

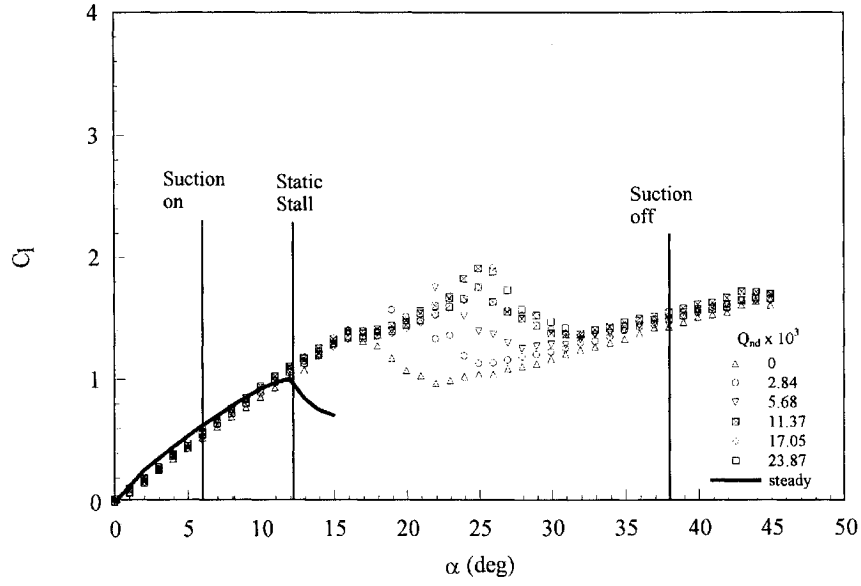

Fig. 9b Effect of suction on the lift coefficient; $\alpha^+ = 0.018$.

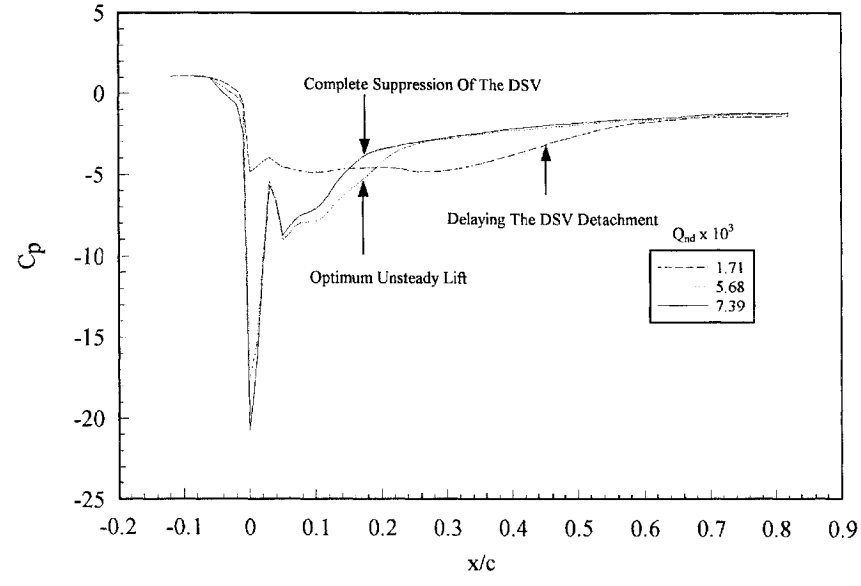

Fig. 10 Surface-pressure distributions for optimum flow state; $\alpha^+ = 0.15$ and $\alpha = 35$ deg.

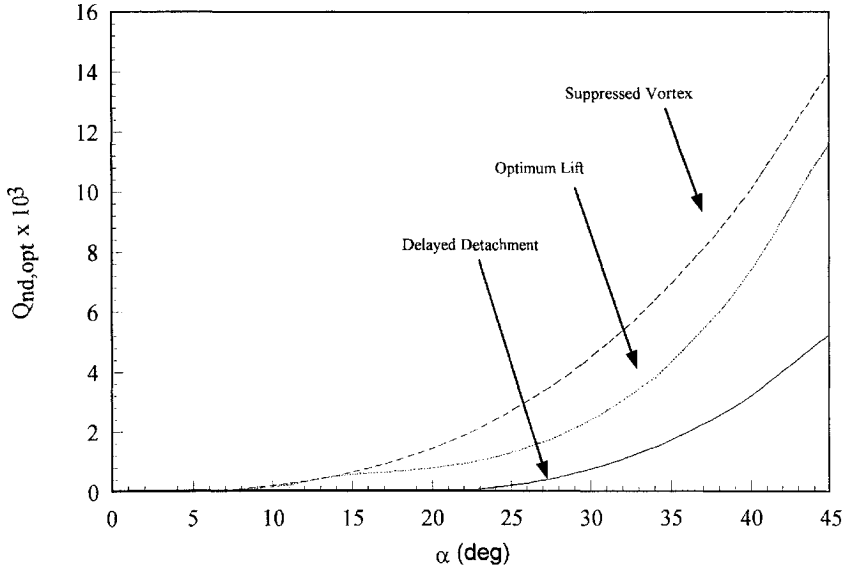

Fig. 11 Optimum suction flow rates for different objectives; $\alpha^+ = 0.15$.

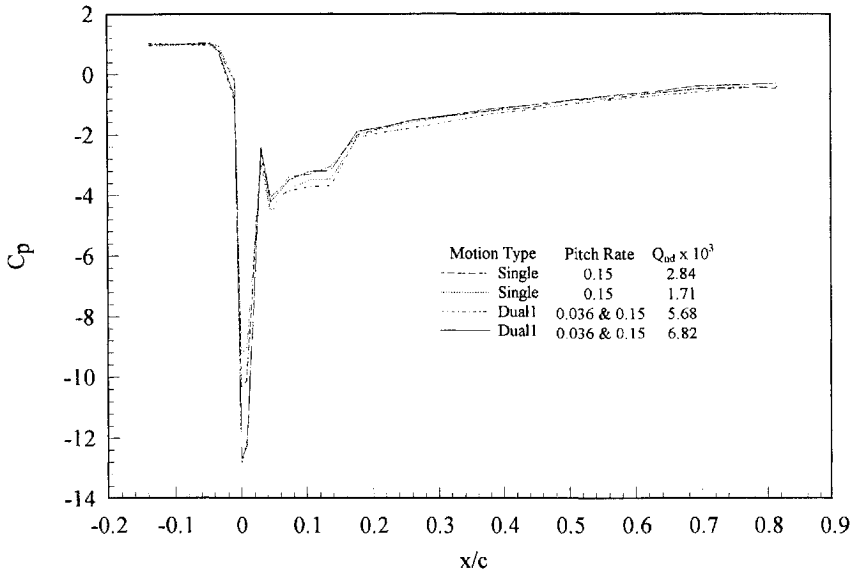

Fig. 12 Surface-pressure distributions for dual-ramp and single-ramp motions; α = 23 deg.

with a single-ramp motion, obtained in the earlier experiments for a range of suction flow rates. A suction flow rate Q_f with the single-ramp motion was determined, for which the pressure distribution matched that obtained in the dual-ramp experiment. Based on the assumption described earlier, it was then argued that the change $\Delta Q = (Q_{opt} - Q_f)$, required at (α, α^+) to suppress the vortex for the simple-ramp motion, would be the same for the dual-ramp case as well; i.e., the suction required to suppress the vortex at that (α, α^+) for the dual-ramp motion would be $Q_i + (Q_{opt} - Q_f)$. The validity of this assumption was investigated at a few angles of attack.

Figure 12 shows the pressure distribution at $\alpha = 23$ deg for a dual-ramp motion with $\alpha^+ = 0.036$ from 0 to 20 deg, $\alpha^+ = 0.15$ from 20 to 45 deg, and $Q_i = 5.68 \times 10^{-3}$. The pressure distributions at $\alpha = 23$ deg for a single-ramp motion with $\alpha^+ = 0.15$ corresponding to $Q_{opt} = 2.84 \times 10^{-3}$ and $Q_f = 1.71 \times 10^{-3}$ are also shown. The dual-ramp pressure distribution for Q_i is very similar to the single-ramp distribution at $Q_f = 1.71 \times 10^{-3}$. The suggested increase in the flow rate to suppress the vortex for the dual-ramp motion is thus $\Delta Q = 1.13 \times 10^{-3}$. A suction flow rate of 6.82×10^{-3} resulted in the same pressure distribution as that at Q_{opt} for the single-ramp motion.

Similar results were obtained for a fast-slow dual-ramp motion with $\alpha^+ = 0.15$ from 0 to 20 deg and $\alpha^+ = 0.036$ from 20 to 45 deg, when compared with single-ramp results at $\alpha^+ = 0.036$. These comparisons validate the assumption stated earlier: the effects of previous history in the airfoil motion and suction flow rate manifest themselves in the state of the flow at any (α, α^+), as reflected in the pressure distribution. If used properly, the results of the present single-ramp motion experiments can be used for other motion and suction histories to determine the change in suction necessary to alter the flow state as desired at that angle of attack. Note that experiments with other motion profiles, including combinations of pitch-up and pitch-down segments, are necessary to ensure that this argument applies for any general motion of the airfoil.

Conclusions

The experiments provided useful information on the behavior of the unsteady pressure field over pitching airfoils with the application of leading-edge suction for flow control. The optimum suction flow rates required to meet three different control objectives were determined, and specifications for the flow state over the airfoil surface to satisfy these objectives were developed. The data were also very

useful in the development of a neural-network controller that can be used to determine the change required in the suction to maintain a suppressed vortex. These results will be used to develop a prototype on-line control system.

Acknowledgments

This research was conducted with the help of Grant F49620-9310106 from the U.S. Air Force Office of Scientific Research, monitored by Daniel Fant and Jim McMichael.

References

[1]Metwally, M. H., "Investigation and Control of the Unsteady Flow over a Pitching Airfoil," Ph.D. Thesis, Mechanical and Aerospace Engineering Dept., Illinois Inst. of Technology, Chicago, IL, Dec. 1990.

[2]Acharya, M., and Metwally, M. H., "Unsteady Pressure Field and Vorticity Production over a Pitching Airfoil," *AIAA Journal*, Vol. 30, No. 2, 1992, pp. 403–411.

[3]Karim, M. A., "Experimental Investigation of the Formation and Control of the Dynamic-Stall Vortex over a Pitching Airfoil," M.S. Thesis, Mechanical and Aerospace Engineering Dept., Illinois Inst. of Technology, Chicago, IL, May 1992.

[4]Acharya, M., Karim, M. A., and Metwally, M. H., "Development of the Dynamic-Stall Vortex over a Pitching Airfoil," *Journal of Fluid Mechanics* (submitted for publication).

[5]Karim, M. A., and Acharya, M., "Suppression of Dynamic-Stall Vortices over Pitching Airfoils by Leading-Edge Suction," *AIAA Journal*, Vol. 32, No. 8, 1994, pp. 1647–1655.

[6]Yang, J., Ghia, K. N., Ghia, U., and Osswald, G. A., "Management of Dynamic Stall Phenomenon Through Active Control of Unsteady Separation," AIAA Paper 93-3284, July 1993.

[7]Kawthar-Ali, M. H., and Acharya, M., "Artificial Neural Networks for Suppression of the Dynamic-Stall Vortex over Pitching Airfoils," AIAA Paper 96-0540, Jan. 1996.

[8]Alrefai, M., "The Unsteady Pressure Field and Flow State over a Pitching Airfoil with Leading-Edge Suction," M.S. Thesis, Mechanical and Aerospace Engineering Dept., Illinois Inst. of Technology, Chicago, IL, Aug. 1995.